Proteomics Characterization of Cell Membrane Blebs in Human Retinal Pigment Epithelium Cells*[S]

Oscar Alcazar‡, Adam M. Hawkridge§, Timothy S. Collier§, Scott W. Cousins¶, Sanjoy K. Bhattacharya‡‖, David C. Muddiman§, and Maria E. Marin-Castano‡**

Age-related macular degeneration (AMD) is the leading cause of legal blindness among the elderly population in the industrialized world, affecting about 14 million people in the United States alone. Smoking is a major environmental risk factor for AMD, and hydroquinone is a major component in cigarette smoke. Hydroquinone induces the formation of cell membrane blebs in human retinal pigment epithelium (RPE). Blebs may accumulate and eventually contribute first to sub-RPE deposits and then drusen formation, which is a prominent histopathologic feature in eyes with AMD. As an attempt to better understand the mechanisms involved in early AMD, we sought to investigate the proteomic profile of RPE blebs. Isolated blebs were subjected to SDS-PAGE fractionation, and in-gel trypsin-digested peptides were analyzed by LC-MS/MS that lead to the identification of a total of 314 proteins. Identified proteins were predominantly involved in oxidative phosphorylation, cell junction, focal adhesion, cytoskeleton regulation, and immunogenic processes. Importantly basigin and matrix metalloproteinase-14, key proteins involved in extracellular matrix remodeling, were identified in RPE blebs and shown to be more prevalent in AMD patients. Altogether our findings suggest, for the first time, the potential involvement of RPE blebs in eye disease and shed light on the implication of cell-derived microvesicles in human pathology. ***Molecular & Cellular Proteomics 8:2201–2211, 2009.***

Age-related macular degeneration (AMD)[1] is one of the most common pathologies in the retina, consisting in a chronic degenerative disorder that constitutes the leading cause of blindness in the elderly, probably affecting 14 million people in the United States. AMD is a multifactorial disease in nature in which age is the predominant risk factor, although there are also environmental factors involved. In this regard, smoking is thought to be a major environmental risk factor as supported by extensive epidemiological evidence (1–5). AMD develops in two different stages: early AMD (also referred to as dry AMD) and the late stage of AMD known as wet AMD by virtue of the extensive neovascularization taking place in the retina choroid. Although there is a fair understanding of the mechanisms involved in wet AMD, little is known about dry AMD and its transition into the most severe stage of this disorder, *i.e.* wet AMD (6).

Early AMD targets the retinal pigment epithelium (RPE) and the Bruch membrane (BrM) in the retina. The RPE constitutes a cell monolayer that is crucial to maintain a normal photoreceptor function. In fact, RPE participates in the cycling of the visual molecules, provides nutrients to rods and cones, and is responsible for withdrawing waste debris from the outer segments of photoreceptors (7). The early stage of AMD is characterized by initial deregulation of the normal extracellular matrix (ECM) turnover leading to thickening of the BrM, sub-RPE deposit accumulation, and drusen formation (8). As mentioned earlier, cumulative evidence suggests that smoking may constitute a major risk factor for early AMD. In fact, we and others have provided evidence that hydroquinone (HQ), a major component of cigarette smoke, has the ability to deregulate the ECM (9–12). Aside from cigarette smoke, HQ is a compound of environmental relevance because of its broad presence in plastics, foodstuff, and air pollution (13, 14).

Mild injuries inflected to the retina elicit a cellular response in the RPE consisting in pinching off small areas of the plasma membrane, which renders small microvesicles called blebs (15). The reason(s) behind membrane blebbing remains unknown, although it has been postulated to be an attempt to discard damaged cellular constituents by the RPE cell (8). Under prolonged injury, blebs may accumulate between the RPE and the basal lamina underneath this cell monolayer. Based on this concept, a plausible role for blebs in the pathogenesis of dry AMD has been suggested as a likely contributor to build-up of the sub-RPE deposits, which are characteristic of the early stages of this disorder (8). To date,

From the ‡Bascom Palmer Eye Institute, University of Miami, Miami, Florida 33136, §W. M. Keck FT-ICR Mass Spectrometry Laboratory, Department of Chemistry, North Carolina State University, Raleigh, North Carolina 27695, and ¶Duke Center for Macular Diseases, Duke University, Durham, North Carolina 27710

Received, April 26, 2009, and in revised form, June 9, 2009

Published, MCP Papers in Press, June 29, 2009, DOI 10.1074/mcp.M900203-MCP200

[1] The abbreviations used are: AMD, age-related macular degeneration; BrM, Bruch membrane; GFP, green fluorescent protein; HQ, hydroquinone; MMP, matrix metalloproteinase; RPE, retinal pigment epithelium; ECM, extracellular matrix; KEGG, Kyoto Encyclopedia of Genes and Genomes; FBS, fetal bovine serum; LTQ, linear trap quadrupole; PNGaseF, peptide:*N*-glycosidase F.

however, RPE bleb composition and potential functions remain largely unexplored.

However, membrane bleb or microvesicle production stimulated by a variety of stress has been extensively described in many different cell types (16–23). To gain a better understanding of the functional relevance of blebs in general and the pathogenic mechanism(s) involved in early AMD in particular, we sought to investigate the identity of proteins carried by human RPE blebs. Previously microvesicles from lymphocytes have been subjected to analysis leading to the identification of a number of proteins (24). In our study, we show the proteomics characterization of stress-induced blebs in RPE cells from human retina. We report identification of several proteins, some of them potentially involved in matrix metalloproteinase (MMP) activation, membrane lipid raft formation, and immunogenic processes. Interestingly RPE blebs were found to carry basigin (including highly glycosylated species) and MMP-14, which are key proteins regulating the ECM turnover and remodeling. A previous proteomics study also has revealed the presence of basigin in the blebs from malignant lymphocytes (24). In the present study, we intended to gain some insight into the functional characterization of blebs to unravel some of the biological consequences of cell membrane blebbing in disease.

EXPERIMENTAL PROCEDURES

Cell Culture and Bleb Isolation—Cell culture materials were purchased from Invitrogen. The human retinal pigment epithelium ARPE-19 cell line was purchased from the American Type Culture Collection (ATCC, Manassas, VA). ARPE-19 cells expressing green fluorescent protein (GFP) were a generous gift from Dr. Csaky (Duke University, Durham, NC). ARPE-19 cells of passages 20–22 were plated at subconfluent density on T-75 (75-cm^2) flasks and grown to confluence in maintenance medium (Dulbecco's modified Eagle's medium-Ham's F-12 (1:1, v/v) supplemented with 10% fetal bovine serum (FBS), 100 μg/ml penicillin/streptomycin, and 0.348% Na_2HCO_3). Cells were maintained at 37 °C in a humidified atmosphere containing 5% CO_2 and 95% air. For the experiments, confluent cells were split, plated at subconfluent density (2×10^5 cells), and grown to confluence. Cells were then prepared for the experiment by changing the maintenance medium to assay medium (*i.e.* maintenance medium without phenol red) for 2 days. This medium was then replaced with assay medium that was supplemented with 1% FBS instead of 10% for 1 day. Subsequently the medium was changed to the assay medium supplemented with 0.1% FBS. At this time, 100 μM HQ was added for 6 h. Conditioned medium was recovered and centrifuged at 100 $\times$ *g* for 15 min at 4 °C. The pellet was washed twice with PBS and centrifuged again at 100 $\times$ *g* for 15 min at 4 °C. Protein content of the pellet was determined using a kit from Bio-Rad based on the Bradford method.

Electrophoretic Separation and Trypsin Digestion—The pellets were suspended in PBS, and protein concentrations were estimated using the Bradford method. Proteins (10 μg) were separated by 4–20% gradient SDS-PAGE (Invitrogen). The gel was stained with GelCode Blue (Pierce); gel slices were excised, destained, reduced with 10 mM DTT for 45 min, alkylated with 55 mM iodoacetamide for 30 min, and digested *in situ* with sequencing grade modified trypsin (0.1 μg/μl; Promega Biosciences Inc., Madison, WI) following protocols routinely used in our laboratory (25, 26); and peptides were subjected to LC MS/MS analysis.

Nanoflow LC-MS/MS—All LC solvents were purchased from Burdick and Jackson (Muskegon, MI). Reversed phase liquid chromatography was performed using a 75-μm-inner diameter PicoFrit capillary column (New Objective, Woburn, MA) with a 15-μm emitter tip packed in house with Magic C18AQ, 5-μm, 200-Å stationary phase (Michrom BioResources, Auburn, CA). The packed volume had dimensions 75-μm inner diameter $\times$ 150 mm and was operated at room temperature. Samples were injected using a PAL Autosampler (LEAP Technologies, Carrboro, NC) and over the course of 10 min trapped and washed on a custom built Magic C18AQ OPTI-PAK trap cartridge (Optimize Technologies, Oregon City, OR) with 100% Mobile Phase A (95:5 water/acetonitrile) at 1 μl/min until a 10-port switching valve (VICI Valco Instruments Co. Inc., Houston, TX) was triggered to move the sample in line with the gradient. Elution was carried out by a Chorus 220 nanoflow pump (CS Analytics, Zwingen, Switzerland) at 500 nl/min with mobile phases containing 95:5 (v/v) (Mobile Phase A) and 5:95 (Mobile Phase B) water and acetonitrile, respectively. The ion pairing reagent used was 0.1% formic acid (Sigma-Aldrich) in both mobile phases. The LC gradient was held at initial conditions of 2% B for 1 min followed by a ramp to 55% B over 45 min, increased to 95% B in 5 min, and held for an additional 3 min before re-equilibrating at 2% B.

Mass spectrometry measurements were performed on a 7-tesla LTQ-FT Ultra instrument from Thermo Scientific (Bremen, Germany). The pulse sequence consisted of five events including a broadband acquisition in profile mode in the ICR cell followed by four data-dependent MS/MS scans in the ion trap. All events used one microscan to determine ionization time to reach the target automatic gain control limit of 5×10^5 in the ICR cell and 3×10^4 in the LTQ. The resolving power of the ICR cell was set at 100,000 full-width half-maximum at $m/z = 400$. MS/MS settings used an isolation width of 2 *m/z* and a normalized collision energy of 35% for a duration of 30 ms. CID was performed on the four most abundant *m/z* values from the precursor ion scan in the LTQ followed by product ion detection. Dynamic exclusion for 60 s was used to reduce redundant analysis of the same precursors.

Data Analysis—Mass Spectrometry data files were subjected to analysis using the BioWorks Browser v3.3 software suite from Thermo Scientific and SEQUEST (27) search algorithm v2.0 against a human proteome database. The human entries in UniProtKB whole proteome database were subjected to searching (53,784 non-redundant entries). For this purpose, the human entries in these database (filename, 25.H_sapiens.fasta) were downloaded in FASTA format from the European Bioinformatics Institute-European Molecular Biology Laboratory and subjected to searching. Data was searched with 5-ppm mass measurement accuracy for peptide precursor ions and 2-amu mass tolerance on fragment ions with variable modifications allowed for methionine oxidation and deamidation of asparagine and glutamine residues. Carboxamidomethylation of cysteine was used as a fixed modification. Up to two missed cleavages were allowed for the digesting enzyme in addition to three modifications per peptide. Identification results were filtered based on XCorr values greater than 1.50, 2.00, and 2.50 for corresponding precursor charge states of 1, 2, and 3, respectively, in addition to peptide probability score (P-score) less than 0.05.

Western Blot—ARPE-19 cells were treated with or without HQ (100 μM, 6 h), and blebs were collected as described earlier. Cell lysates and conditioned media were collected. Total protein concentration was determined using a kit based on the Bradford method (Bio-Rad). Twenty micrograms of protein extracts were denatured in Laemmli sample buffer followed by 5 min of boiling and then resolved on a 4–20% Tris-glycine gel (Novex, San Diego, CA). After electrophoresis

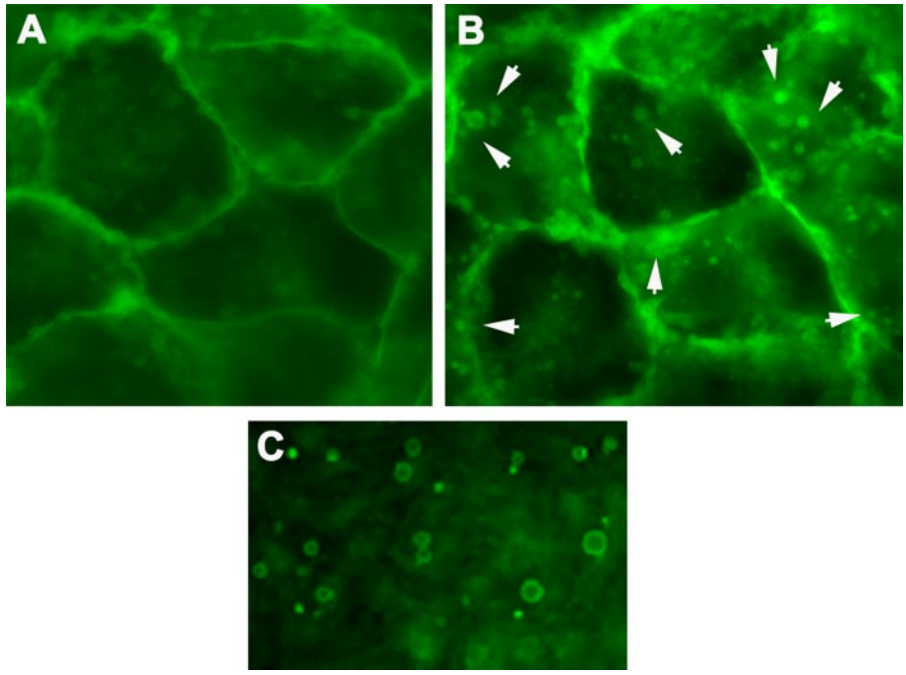

FIG. 1. **Induction of membrane blebs in ARPE-19 cells by hydroquinone-induced cellular stress.** ARPE-19 cells expressing GFP at the plasma membrane (*A*) were exposed to HQ (100 μM) for 6 h (*B*). Cells were observed immediately under epifluorescence microscope (*magnification*, ×40). The figure shows GFP localized to the membrane and the presence of membrane blebs (*white arrowheads*) after HQ treatment. A detailed view of the blebs that accumulated in the conditioned medium after HQ treatment is shown (*C*).

(120 V for 2 h), proteins were transferred in 1× transfer buffer (25 mM Tris, 192 mM glycine, 0.1% SDS, and 20% methanol (pH ~ 8.4)) to a Hybond-ECL nitrocellulose membrane (Amersham Biosciences) using constant current (100 mA) for 2 or 3 h. Membranes were blocked in 5% nonfat dry milk, TBS solution for 1 h at room temperature. Blots were incubated overnight at 4 °C with either mouse polyclonal anti-basigin (Novus Biologicals, Littleton, CO) or mouse monoclonal anti-MMP-14 (Chemicon, Temecula, CA) antibodies. Membranes were washed three times with TBS solution including Tween 20 (TBS-T), incubated with horseradish peroxidase-linked donkey anti-mouse antibody (Santa Cruz Biotechnology, Santa Cruz, CA) for 2 h at room temperature, and then washed four times in TBS-T. Detection was performed with the chemiluminescent reagent luminol (Santa Cruz Biotechnology).

Peptide:N-glycosidase F (PNGaseF) Digestion—PNGaseF (New England Biolabs, Ipswich, MA) was used according to the manufacturer's instructions. Briefly lysate samples (20 μg of total protein) were acetone-precipitated following standard protocols (28) and resuspended in 9 μl of PBS. Samples were boiled for 10 min in a final volume of 10 μl after addition of 1 μl of denaturation buffer provided with the PNGaseF. Denatured samples were added to the reaction solution (1% Nonidet P-40 in 50 mM sodium phosphate at pH 7.5) in a 20-μl final volume. Each sample was split into two: one-half was treated with PNGaseF (25 units/μg of protein), and the other half was untreated (control). PNGaseF-treated and control solutions were incubated at 37 °C for 1 h and finally subjected to Western blot analysis.

MMP-2 Activity—Conditioned culture medium was collected after treatment and clarified by centrifugation at 15,000 × *g* for 30 min at 4 °C. Protein concentration was determined, and MMP-2 activity was assessed using 10% gelatin zymography gels (Novex). Ten micrograms of protein extracts were subjected to electrophoresis (120 V for 2 h) and subsequently incubated in 2.5% Triton X-100 for 1.5 h. Gels were next incubated in 50 mM Tris buffer for 18 h, allowing determination of total proteolytic MMP-2 activity with no interference from their associated tissue inhibitors. Gels were stained using a Brilliant Blue R solution (Sigma-Aldrich) for 2 h. Densitometry was performed using Image J 1.17 software (National Institutes of Health, Bethesda, MD).

Immunohistochemistry—Serial cross-sections of human donor eyes were obtained from the National Disease Research Interchange. They were deparaffinized and incubated in blocking solution (5% BSA and 1% Triton X-100) for 1 h. Thereafter sections were examined for the presence of basigin and MMP-14 using overnight incubation with mouse polyclonal anti-basigin (1:500; Novus Biologicals) or mouse monoclonal anti-MMP-14 (1:500; Chemicon) antibodies, respectively. Eye sections were then incubated for 2 h using an anti-mouse Alexa Fluor 488-conjugated (1:500; Invitrogen) secondary antibody. Cell nuclei were stained with 4,6-diamidino-2-phenylindole dihydrochloride (1:5000; Invitrogen) for 5 min. Stained sections were mounted, and images were viewed at 40× magnification using a dual channel laser scanning confocal microscope (Leica, Exton, PA). Images were digitally acquired, and the figure was composed using image-managing software (Photoshop CS, Adobe, San Jose, CA).

RESULTS

RPE Bleb Induction and Isolation—ARPE-19 is a human immortalized cell line that is widely used as an RPE model *in vitro* (29). Previous studies by our laboratory have shown that stress induced with HQ (100 μM) for 6 h resulted in membrane bleb formation without compromising cell viability in ARPE-19 cells (10, 11).

To monitor bleb formation under the established HQ treatment conditions (100 μM, 6 h), ARPE-19 cells genetically modified to express GFP were utilized. These cells express a fusion protein of GFP with a small G protein fragment that targets GFP to the plasma membrane (12). Therefore, membrane bleb formation can be easily visualized under an epifluorescence microscope.

Non-treated, control ARPE-19 cells generated only a reduced number of blebs. However, incubation with HQ (100 μM) for 6 h notably increased the amount of membrane-generated blebs (Fig. 1). A survival curve using different times

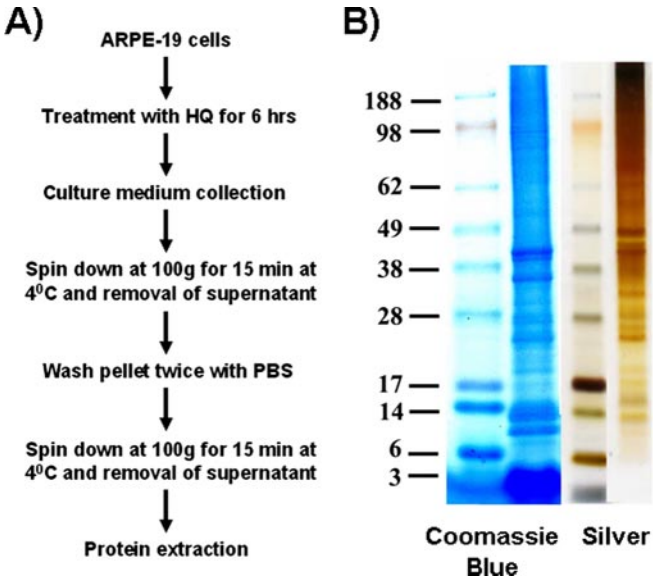

FIG. 2. **Isolation of blebs.** *A*, scheme for bleb isolation. ARPE-19 cells were treated with HQ (100 μM) for 6 h. Culture medium was collected and centrifuged at 100 $\times$ *g* for 15 min at 4 °C. The resulting pellet was washed twice with PBS and resuspended. The resuspended pellet was centrifuged at 100 $\times$ *g* for 15 min at 4 °C, and the supernatant was removed. Blebs were collected and used for protein extraction. *B*, representative one-dimensional gel showing the Coomassie Blue and silver stainings of resolved proteins present in ARPE-19 blebs.

of exposure to HQ (100 μM) confirmed that cell viability remained unaffected (data not shown).

The protocol to isolate blebs is described under "Experimental Procedures" and outlined as a scheme in Fig. 2*A*. A large volume of cultured ARPE-19 cells treated with HQ was required to obtain the amount of protein necessary to perform this study. Cultured cells were adequately monitored to assure the absence of apoptosis, which might have contaminated the bleb population with apoptotic bodies.

Staining of RPE Bleb Proteins—RPE bleb proteins were fractionated on one-dimensional rather than two-dimensional SDS-PAGE. Based on the scarcity of the biological material (RPE blebs), it was not advisable to resolve proteins by two-dimensional SDS-PAGE to minimize protein loss (30–32).

The RPE bleb protein profile was analyzed by loading 10 μg of total proteins and using two different stains, *i.e.* Coomassie Blue and silver. Silver staining is more sensitive than Coomassie and allowed detection of more bands (Fig. 2*B*). However, some proteins were only selectively stained by Coomassie and not shown with the silver staining procedure. The combined use of both staining methods (Coomassie and silver) assures the detection of bands that are specifically recognized by one reagent but not by the other. Prominent bands were detected at ~36 and 40 kDa (two bands), 10 and 14 kDa (two bands), and ≤3 kDa (single broad band) with Coomassie Blue. The identity of proteins in this lower molecular mass broad band is likely to be statherin and histatin among others, which are salivary calcium-bound phosphoproteins. Staining total proteins with silver stain showed some major additional bands in the approximately 25–50-kDa region but failed to reveal any protein in the lower molecular mass region, that is ≤3-kDa proteins (Fig. 2*B*).

Identification of RPE Bleb Proteins—LC-MS/MS of in-gel trypsin-digested RPE bleb proteins identified a total of 314 proteins (supplemental data). Selected proteins with at least two peptide matches with good spectra are shown in Table I. Proteins identified were subjected to functional clustering analysis by using the Kyoto Encyclopedia of Genes and Genomes (KEGG) pathway database (Fig. 3). This functional characterization of proteins from blebs yielded glycolysis, oxidative phosphorylation, cell junction, and actin cytoskeleton regulation as the cellular pathways whose members are more frequently featured in RPE blebs. Focal adhesion, leukocyte transendothelial migration, and antigen processing and presentation were also potentially interesting categories represented in RPE blebs. To complement the information provided by KEGG, a pathway network MetaCore analysis was performed using the GeneGO portal for examination of potential regulatory networks related to proteins identified in the RPE blebs. Cell adhesion and immune response were some relevant cell processes highlighted by the MetaCore analysis on the proteins detected by LC-MS/MS in blebs (Table II).

Interestingly basigin and MMP-14 were identified in the RPE blebs. Both proteins are of especial relevance to the dry AMD pathology as they promote MMP-2 activation, which is a key enzyme involved in the RPE extracellular matrix remodeling.

Western Blot Analysis—To validate the results of the proteomics profiling, semiquantitative Western blot analysis of basigin and MMP-14 was performed. Non-treated, control ARPE-19 cells, HQ-treated ARPE-19 cells, and membrane blebs generated after HQ-induced stress were analyzed (Fig. 4*A*). The basigin immunoblot showed a double band pattern, *i.e.* a thin, lower molecular weight band that corresponds to the non-glycosylated basigin and a wide, higher molecular weight band that represents basigin highly glycosylated to different degrees. Importantly blebs were shown to harbor highly glycosylated basigin, which is the type of post-translational modification that confers basigin its ability to induce MMP activity. To verify that the upper band of basigin is the result of glycosylation, we subjected proteins extracted from the RPE membrane blebs to digestion with the enzyme PNGaseF, which cleaves carbohydrate residues from *N*-linked glycoproteins. Western blot analysis showed the disappearance of the upper, broad band of basigin after digestion with PNGaseF (Fig. 4*B*). Altogether the results confirmed that both (highly glycosylated) basigin and MMP-14 were carried by the RPE membrane blebs.

Immunohistochemical Analysis—To corroborate in human tissue the expression of basigin and MMP-14 found in the

TABLE I
Selected proteins identified in human RPE blebs by LC-MS/MS analysis

Accession number[a]	Protein name	Molecular mass	Peptide matches	Sequence coverage
		kDa		%
P31937	3-Hydroxyisobutyrate dehydrogenase	35	5	28
O43707	Actinin, α4	104	12	21
P84085	ADP-ribosylation factor 5	20	6	43
P04075	Aldolase A	39	7	29
P04083	Annexin I	38	14	61
P08758	Annexin 5	36	8	54
Q99700	Ataxin 2	140	2	6
P35613	Basigin	42	6	28
P62158	Calmodulin 3	17	3	36
P21926	CD9 antigen	25	3	10
P16070	CD44 antigen	81	15	32
P08962	CD63 antigen	26	7	33
P60033	CD81 antigen	26	2	20
Q00610	Clathrin heavy chain 1	191	16	14
Q07065	Cytoskeleton-associated protein 4	66	11	28
P17661	Desmin	53	11	36
P68104	Elongation factor 1 α1	50	6	24
Q14254	Flotillin 2	47	7	23
P06744	Glucose-phosphate isomerase	63	2	10
P09211	Glutathione transferase	23	2	21
P04406	Glyceraldehyde-3-phosphate dehydrogenase	36	7	38
NP_057406	GTPase Rab 14	24	2	20
P38646	Heat shock 70-kDa protein 9B precursor	73	2	10
P08729	Keratin 7	51	10	33
P05783	Keratin 18	48	17	57
P00338	Lactate dehydrogenase A	37	10	39
NP_733821	Lamin A/C isoform 1 precursor	74	8	23
Q8IVL6	Leprecan-like 2	82	2	7
P50281	Matrix metalloproteinase-14	66	9	25
Q9BYN8	Mitochondrial ribosomal protein S26	24	4	34
O00483	NADH dehydrogenase subunit 4	51	4	17
Q9Y2G5	*O*-Fucosyltransferase 2 isoform C	50	5	25
NP_000933	Peptidylprolyl isomerase B precursor	24	7	38
NP_857635	Peroxiredoxin 5 precursor, isoform c	13	5	46
Q96S52	Phosphatidylinositol glycan class S	62	2	10
Q00169	Phosphatidylinositol transfer protein, α	32	5	36
P61019	RAB2A, member RAS oncogene family	23	2	18
P39019	Ribosomal protein S19	16	2	22
O75396	SEC22 vesicle trafficking protein homolog B	25	4	33
Q15019	Septin 2	41	6	30
P12236	Solute carrier family 25, member A6	33	5	25
Q16881	Thioredoxin reductase 1	54	12	33
Q71U36	Tubulin α1a	50	5	18
Q9Y277	Voltage-dependent anion channel 3	31	5	33

[a] Swiss-Prot database accession numbers are shown.

human cell line ARPE-19, eye sections from eye donors were subjected to immunohistochemical analysis (Fig. 5). Negative controls for the immunostaining were obtained by omission of the primary antibody (Fig. 5, *A* and *B*). Expression of basigin was shown to be confined to the RPE in a normal, healthy retina (Fig. 5*C*). In contrast, the retina of a dry AMD eye revealed a widespread basigin staining, including the BrM and even the choroid areas, consistent with the hypothesis that blebs might carry typical RPE proteins to distal locations (Fig. 5*D*). Similarly MMP-14 expression was predominantly located at the RPE in a normal, healthy retina (Fig. 5*E*). Interestingly like basigin, MMP-14 immunostaining of a dry AMD retina showed extensive expression of this protein although at lower intensity than basigin (Fig. 5*F*).

Gelatinase Activity by MMP-2—To gain some insight into the potential physiological relevance of the basigin and MMP-14 proteins carried by blebs, ARPE-19 cells were incubated with isolated blebs for 24 h, and MMP-2 activity was assessed. Interestingly MMP-2 activity significantly increased in the conditioned medium containing blebs (Fig. 6). A dose-

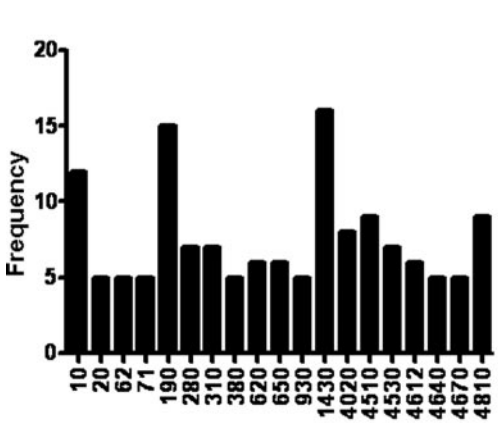

KEGG #	Pathway
10	Glycolysis
20	TCA
62	Fatty acid elongation (mitochondria)
71	Fatty acid metabolism
190	Oxidative phosphorylation
280	Val, Leu, Ile degradation
310	Lys degradation
380	Trp metabolism
620	Pyruvate metabolism
650	Butanoate metabolism
930	Caprolactam degradation
1430	Cell junction
4020	Calcium signaling
4510	Focal adhesion
4530	Tight junction
4612	Antigen processing and presentation
4640	Hematopoietic cell lineage
4670	Leukocyte transendothelial migration
4810	Actin cytoskeleton regulation

FIG. 3. **Functional characterization of proteins identified in hydroquinone-induced blebs.** The distribution profile of the proteins identified in hydroquinone-induced blebs is depicted according to functional categories. The KEGG database number and its corresponding metabolic pathway are shown. *TCA*, tricarboxylic acid cycle.

TABLE II

Cell processes associated to selected proteins identified in RPE blebs by GeneGO MetaCore pathway analysis

MCH, major histocompatibility complex; BCR, B cell receptor; NK, natural killer; ICOS, inducible co-stimulator; ICOSL, ICOS ligand; NFAT, nuclear factor of activated T cells

Map	Cell process	*p* value	Objects[a]
Endothelial cell contacts by non-junctional mechanisms	Cell adhesion	9.98*e*−06	10, 70
Integrin-mediated cell adhesion	Cell adhesion	6.20*e*−05	12,122
Antigen presentation by MHC class I	Immune response	1.41*e*−04	9, 77
Tetraspanins in integrin-mediated cell adhesion	Cell adhesion	4.20*e*−04	10,108
Integrin inside-out signaling	Cell adhesion	1.29*e*−02	8,122
Endothelial cell contacts by junctional mechanisms	Cell adhesion	3.23*e*−01	3, 78
CCR3 signaling in eosinophils	Immune response	3.97*e*−01	5,161
CCR4-induced leukocyte adhesion	Cell adhesion, immune response	4.84*e*−01	2, 63
Function MEF2 in T lymphocytes	Immune response	7.92*e*−01	2,113
Leukocyte chemotaxis	Cell adhesion, immune response	7.94*e*−01	3,163
BCR pathway	Immune response	8.39*e*−01	2,126
CD16 signaling in NK cells	Immune response	9.30*e*−01	2,166
ICOS-ICOSL pathway in T- helper cell	Immune response	9.36*e*−01	1,105
NFAT in immune response	Immune response	9.38*e*−01	1,106
Role of integrins in NK cells cytotoxicity	Immune response	9.44*e*−01	1,110
CD28 signaling	Immune response	9.45*e*−01	1,111

[a] The first number represents positive links to other nodes in the pathway network. The second number refers to negative links.

response study was first established to determine an adequate bleb dose inducing a clear increase in MMP-2 activity (Fig. 6*A*). The number of blebs was determined using a Z1 Coulter Particle Counter (Beckman Coulter, Fullerton, CA), and 5×10^5 blebs/4.5×10^5 cells were set as the bleb dose for subsequent experiments. To discard the possibility that isolated blebs might carry over contaminating MMP-2 enzyme accounting for the observed elevation in MMP-2 activity, isolated blebs were analyzed in the absence of cells. Using conditioned media from non-treated cells and HQ-treated cells as controls, we could verify that the isolated bleb preparation was barely carrying any MMP-2 contaminating activity (Fig. 6*B*). MMP-2 activity was next assayed by treating ARPE-19 cells with anti-basigin (1:500) and anti-MMP-14 (1:500) antibodies alone or combined in the presence or absence of isolated blebs (Fig. 6*C*). Incubation of ARPE-19 cells with isolated blebs induced a significant increase of approximately 50% in MMP-2 activity. Neither anti-basigin nor anti-MMP-14 antibody alone changed the MMP-2 activity base line. However, when added separately to the cells incubated with blebs, the increase in MMP-2 activity was reduced. Moreover combination of anti-basigin and anti-MMP-14 antibodies together completely blunted the bleb effect on MMP-2 activity (Fig. 6*C*).

DISCUSSION

AMD is a late onset, progressive degeneration of the retina associated with vision loss due to retinal photoreceptor dysfunction. However, the initial pathogenic target of AMD is the RPE (6, 8). AMD progresses through two stages: early and late. Early AMD ("atrophic" or "dry" degeneration) is characterized by accumulation of various lipid-rich extracellular de-

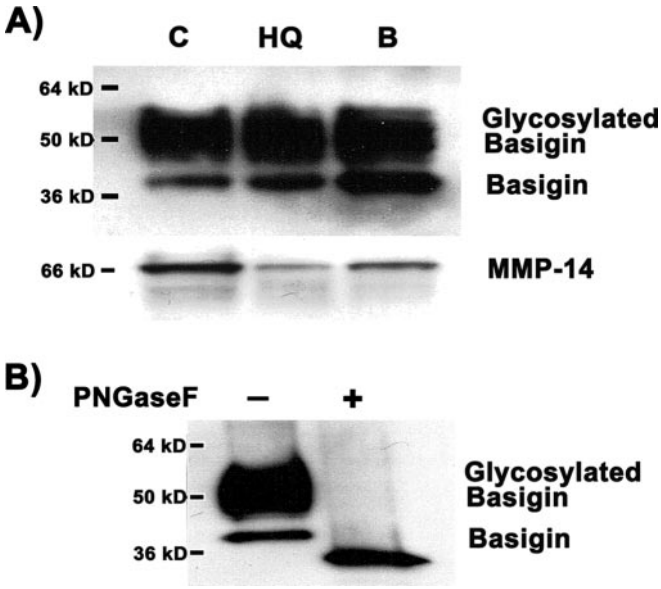

FIG. 4. **Western blot analysis of basigin and MMP-14 expression in hydroquinone-induced blebs.** Protein expression was analyzed in 20 μg of total ARPE-19 cell lysate. *A*, basigin and MMP-14 expression in control, untreated cells (*C*), cells treated with 100 μM HQ for 6 h (*HQ*), and isolated HQ-induced membrane blebs (*B*). Basigin analysis shows a higher molecular mass, broad band corresponding to highly glycosylated species of basigin. *B*, Western blot analysis of basigin in isolated HQ-induced membrane blebs before and after digestion with the enzyme PNGaseF, which selectively removes *N*-linked carbohydrate residues. The blot from a representative experiment is shown. The *number* on the *left* represents the molecular mass of the protein.

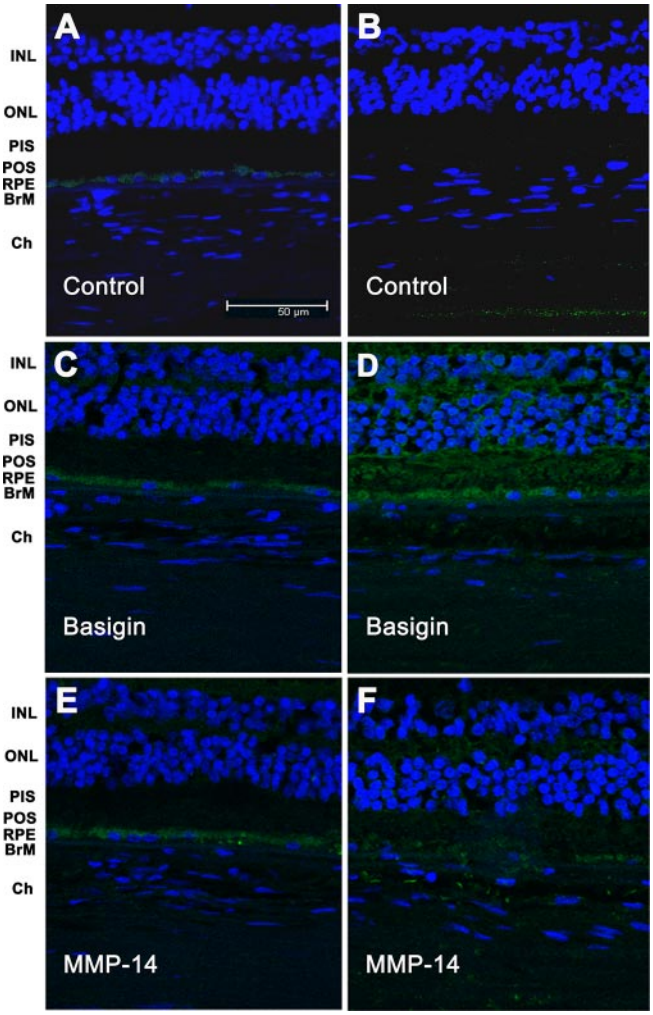

FIG. 5. **Immunohistochemical analysis of basigin and MMP-14 in human retina.** Retina sections from human donor eyes with no known eye disease (*A*, *C*, and *E*) or from human donor eyes with dry AMD (*B*, *D*, and *F*) were stained with either mouse polyclonal anti-basigin (*C* and *D*) or mouse monoclonal anti-MMP-14 (*E* and *F*) as indicated. Negative controls were generated by omission of the primary antibody (*A* and *B*). Secondary antibodies were coupled to Alexa Fluor 488. Nuclei were stained with 4,6-diamidino-2-phenylindole dihydrochloride. Sections were analyzed under a confocal microscope. *INL*, inner nuclear layer; *ONL*, outer nuclear layer; *PIS*, photoreceptor inner segments; *POS*, photoreceptor outer segments; *Ch*, choroid.

posits under the RPE, and the late form of AMD ("exudative" or "wet" degeneration) is characterized by endothelial invasion and pathological neovascularization under the retina (33). Wet AMD is always preceded by early disease. The accumulation of specific deposits between the RPE and BrM is a very prominent histopathologic feature that constitutes the earliest clinical hallmark of AMD (8, 34). These deposits are generically termed "drusen" and are known to be contributed by RPE membrane blebs (35–38).

Our study describes for the first time the characterization of cell membrane blebs generated by the RPE under situations of cellular stress using a proteomics approach. We performed our study utilizing the widely used human ARPE-19 cell line. Protein content profiling confirmed that blebs are microvesicles composed of plasma membrane including cytosol and probably some organelles. The presence of proteins bound to the plasma membrane as well as proteins participating in typical cell metabolic processes occurring in the cytosol and in organelles (*e.g.* mitochondrion) supported this view. Although we analyzed the RPE blebs for the first time, membrane blebs from other systems such as from lymphocytes have already been subjected to proteomics analysis (24).

An intriguing question about RPE blebs refers to their origin, whether they can be generated indistinctly in the plasma membrane or rather from specialized membrane microdomains. The proteomics characterization of RPE blebs revealed the presence of flotillin 2, also called reggie 1, which is a cytoplasmic protein associated to the plasma membrane that defines lipid rafts microdomains of non-caveolar nature (39, 40). Lipid rafts are membrane microdomains enriched in cholesterol and sphingolipids that concentrate a number of signaling molecules within the cell (41–43). There are two different families of lipid-binding proteins that orchestrate the organization of lipid rafts: caveolins and flotillins. Although caveolins are more devoted to regulating cholesterol traffick-

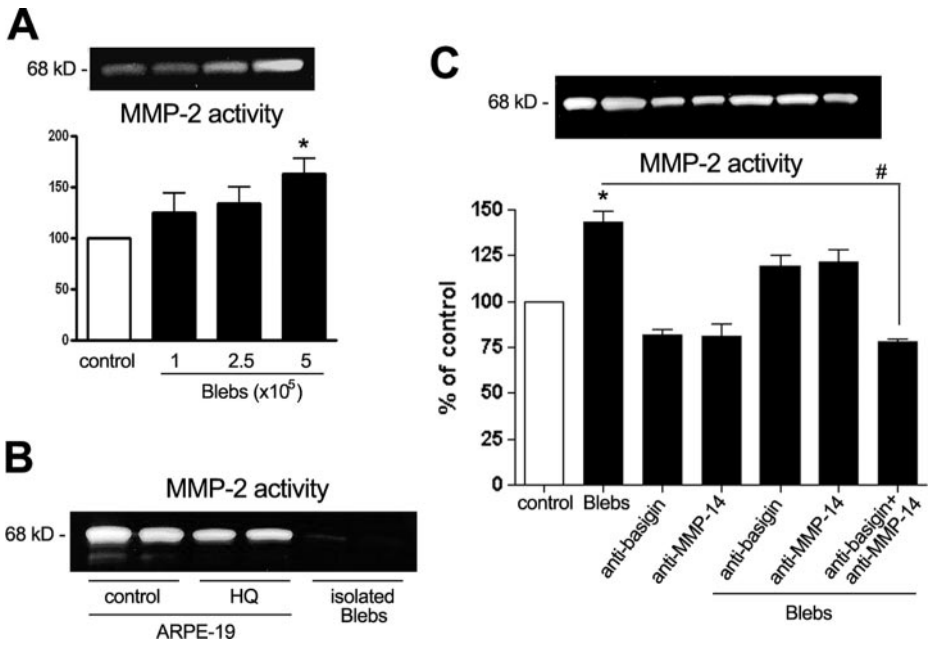

FIG. 6. **MMP-2 activity in ARPE-19 cells exposed to hydroquinone-induced blebs.** Blebs were generated by incubation with 100 μM HQ for 6 h and used to treat ARPE-19 cells for 24 h. Thereafter conditioned medium was collected, and MMP-2 activity was evaluated by gelatin zymography. *A*, MMP-2 activity from cells (4.5×10^5) incubated with increasing concentrations of blebs. *B*, MMP-2 activity in control, non-treated cells (*C*), HQ-treated cells (*HQ*), and isolated blebs alone (*B*). *C*, MMP-2 activity from cells incubated with blebs (5×10^5 blebs/4.5×10^5 cells) in the presence or absence of anti-basigin (1:500) and anti-MMP-14 (1:500) antibodies. *Top*, gelatin zymogram from a representative experiment. *Bottom*, bar graph showing averages of results of three independent experiments. Results are expressed as mean ± S.E. #, $p < 0.01$; *, $p < 0.05$ compared with control cells. *Error bars* indicate standard error of the mean.

ing and distribution, flotillins are mainly implicated in cellular signaling events (39, 44). The fact that the protein caveolin was not found in the blebs excludes the possibility that caveolae might be present in the blebs. However, the presence of flotillin 2 in blebs suggested the possibility that non-caveolar lipid rafts might be involved in the blebbing process. Further investigation is required to validate this hypothesis by analyzing whether RPE bleb membranes are enriched in cholesterol and other lipids particularly abundant in lipid rafts. If so, the possibility exists that specialized membrane microdomains might be implicated in the generation of blebs in RPE cells.

An interesting protein detected in our RPE bleb study was basigin, which has been reported previously in malignant lymphocytes (24). A previous proteomics analysis first described the occurrence of basigin among an array of 17 CD antigens expressed in the plasma membrane. Our finding of basigin in blebs that originated from a completely different cell type (RPE cells) opens the question as to whether there is especial relevance of the presence of basigin in blebs/microvesicles irrespective of the originating cell or tissue.

Basigin, also referred to as CD147 or EMMPRIN (extracellular matrix metalloproteinase inducer), is a cell surface transmembrane protein that belongs to the immunoglobulin superfamily and can be heavily glycosylated (45, 46). This protein has been associated to a number of pathological states, especially induction of MMP synthesis, angiogenesis, and cell proliferation in cancer cells (47–50). Interestingly MMP-2 and MMP-14 are listed among the MMPs that basigin induces (51–55); MMP-2 and MMP-14 are the major proteins involved in the degradation and remodeling of the ECM in retina. In fact, there is evidence that an imbalance in MMP-2 activity may play a critical role during the early stages of AMD in the RPE-choroid (11).

Only the glycosylated form of basigin is able to induce the activity of MMPs (56), and our study revealed that RPE blebs carry highly glycosylated basigin. Basigin can modulate MMP activity by varying the level of glycosylation independently of the MMP *de novo* synthesis. In fact, the molecular mass for the unglycosylated form of basigin is about 30 kDa, and it is increased in variable amounts up to 50–60 kDa depending on the degree of glycosylation (46). Gel staining for glycoproteins showed a heavily glycosylated band at approximately 62 kDa consistent with the possibility that basigin might be glycosylated in RPE blebs (data not shown). This gel band was excised and analyzed by LC-MS/MS, confirming the presence of basigin in a molecular weight range proper for highly glycosylated species of this protein (data not shown). Moreover expression of basigin and its highly glycosylated forms was further confirmed by Western blot analysis in RPE blebs after digestion of the carbohydrate residues with the enzyme PNGaseF. This finding suggests that basigin carried by RPE blebs may potentially exhibit pathological relevance as highly glycosylated species of this protein may activate MMPs, which in turn would favor ECM degradation. It is tempting to speculate that bleb-carried basigin might increase MMP-2 activity in the proximity of the basement membrane, allowing the blebs to migrate from the RPE toward the BrM, contributing to the progression of dry AMD.

To explore this hypothesis, we evaluated the expression of basigin on human retina flat mount preparations by immunofluorescence in healthy and dry AMD retina sections. Basigin was shown to be predominantly expressed in the RPE of normal retina, whereas its expression was highly disseminated in the dry AMD retina including the BrM area consistent with the possibility of a bleb-mediated transport of basigin distal to RPE. The fact that a second protein (MMP-14) that is

also predominantly expressed in the RPE displayed a similar distribution pattern in dry AMD retina sections supported this view.

Notably there is evidence in nonocular tissues that basigin may be transported through microvesicles that are later degraded, releasing full-length soluble, active basigin (57). This proposed mechanism may have profound consequences in physiology as it permits basigin to exert its actions at distant sites. In this context, MMP-14 was an interesting candidate for the basigin shedding as our study found this protein to be carried by the RPE blebs along with basigin as assessed by proteomics and Western blot analyses. This view is supported by a recent study that provides evidence that MMP-14 seems to be responsible for the cell-mediated shedding of basigin in tumor cells (58).

The Western blot analysis of MMP-14 revealed a lower level of expression of this protein in cells incubated with HQ (Fig. 4*A*). This finding might be explained by a partial decrease of cellular MMP-14 content due to the loss of MMP-14 in the blebbing process. The occurrence of flotillin 2 in the HQ-induced RPE blebs, suggesting that they might be generated in lipid rafts, and evidence in other cell types that MMP-14 appears associated to these microdomains support this view (59–61). The loss in MMP-14 might account, at least in part, to the observed decrease in MMP-2 activity after incubating ARPE-19 cells with HQ (Fig. 6*B*), an effect that has been reported previously (9, 11).

To better understand the potential role played by bleb-carried basigin and MMP-14 in retinal disease, we incubated ARPE-19 cells with conditioned medium containing blebs and observed an increase in MMP-2 activity. This finding clearly supports the view that basigin and MMP-14 carried by blebs are biologically active and thereby physiologically relevant. Moreover incubation with either anti-basigin or anti-MMP-14 antibodies limited the increase in MMP-2 activity, whereas combined incubation with both antibodies completely abrogated the effect of the blebs on MMP-2 activity. This finding constitutes evidence that basigin and MMP-14 carried by RPE membrane blebs may play an important role modulating MMP-2 activity *in vitro*. As a consequence, the possibility exists that blebs may induce deregulation of normal ECM remodeling events and thereby participate in pathological processes. This may be especially relevant to any cell type/tissue where basigin is carried by blebs. Further investigation is necessary to confirm in animal models these observations *in vitro*.

Members of a family of proteins called Tetraspanins were also detected by our proteomics analysis of RPE blebs. In particular, our study showed that CD9, CD44, CD63, and CD81 were present in RPE blebs (Table I). This superfamily of proteins are cell surface glycoproteins featuring a typical topology of four transmembrane domains and two extracellular regions (62). Tetraspanins are known to be implicated in biological processes such as cell adhesion, migration, co-stimulation, signal transduction, and differentiation (63–65). From these glycoproteins, at least CD9 and CD63 may exert immunogenic properties, opening the possibility that, aside from participating in ECM remodeling processes, RPE blebs might also exhibit the ability to trigger an immunologic response.

Production of cell membrane microvesicles has been documented previously in blood cells (monocytes, neutrophils, erythrocytes, and platelets) subjected to stimulation with lipopolysaccharide or sublytic complement as well as in endothelial and renal glomerular epithelial cells (16–21). These studies have provided evidence that the originated microvesicles are often coated with proteins that are able to confer procoagulant and even proadhesive properties. Additional studies performed on erythrocytes have extended this array of microvesicle functions suggesting relevance to inflammation (22, 23). Microvesicles that are shed from cells have often been generically termed as ectosomes and proposed to constitute a sorting mechanism to disseminate proteins that may be relevant to some pathological disorders. In this regard, RPE blebs might resemble the so-called ectosomes, which seem to be involved in promoting processes of inflammation and coagulation. From our proteomics analysis it is not possible to assure that RPE blebs are ectosomes given that different cell types seems to exhibit distinct arrays of proteins in their microvesicles. However, RPE blebs might be considered as ectosome-like microvesicles if it is confirmed that they have the ability to elicit specific immune responses. Interestingly the *in silico* GeneGO MetaCore analysis performed on our RPE bleb proteomic profile supported this view by predicting a number of putative processes of cell adhesion and immune response associated to RPE blebs (Table II). Demonstration that RPE blebs may contribute to the local recruitment of immune cells and/or exacerbation of inflammatory events would represent at least in part a potential mechanism to explain the transition from early (dry) AMD to late (wet) AMD. Ongoing experiments are aimed at confirming immunogenic properties of RPE blebs in our laboratory.

In conclusion, the present study provided a proteomics characterization of RPE blebs that revealed the presence of proteins previously reported in the microvesicles from other systems. Glycosylated forms of basigin and MMP-14 present in blebs might be involved in ECM remodeling processes at distal sites from the RPE, potentially contributing to the progression of dry AMD. Indeed we found evidence that basigin and MMP-14 expression may be increased in AMD patients. Moreover we showed evidence for the first time that blebs are capable of altering MMP-2 activity *in vitro*. The presence of basigin in RPE and lymphocyte blebs (24) perhaps suggests that its presence is a general property of these vesicles irrespective of the originating cell/tissue.

* This work was supported, in whole or in part, by National Institutes of Health Grants R01-EY015249-01A1, EY015249-01A1S1, and P30-EY14801. This work was also supported by an unrestricted grant from Research to Prevent Blindness (RPB) and an RPB career award (to S. K. B.).

S The on-line version of this article (available at http://www.mcponline.org) contains supplemental material.

‖ To whom correspondence may be addressed: Ocular Proteomics Laboratory, Bascom Palmer Eye Inst., University of Miami, 1638 N. W. 10th Ave., Miami, FL 33136. Tel.: 305-482-4103; E-mail: SBhattacharya@med.miami.edu.

** To whom correspondence may be addressed: Center for Molecular Ophthalmology, Bascom Palmer Eye Inst., University of Miami, 1638 N. W. 10th Ave., Miami, FL 33136. Tel.: 305-547-3660; E-mail: MCastano@med.miami.edu.

REFERENCES

1. Christen, W. G., Glynn, R. J., Manson, J. E., Ajani, U. A., and Buring, J. E. (1996) A prospective study of cigarette smoking and risk of age-related macular degeneration in men. *JAMA* **276,** 1147–1151
2. Clemons, T. E., Milton, R. C., Klein, R., Seddon, J. M., and Ferris, F. L., 3rd (2005) Risk factors for the incidence of Advanced Age-Related Macular Degeneration in the Age-Related Eye Disease Study (AREDS) AREDS report no. 19. *Ophthalmology* **112,** 533–539
3. Evans, J. R. (2001) Risk factors for age-related macular degeneration. *Prog. Retin. Eye Res.* **20,** 227–253
4. Khan, J. C., Thurlby, D. A., Shahid, H., Clayton, D. G., Yates, J. R., Bradley, M., Moore, A. T., and Bird, A. C. (2006) Smoking and age related macular degeneration: the number of pack years of cigarette smoking is a major determinant of risk for both geographic atrophy and choroidal neovascularisation. *Br. J. Ophthalmol.* **90,** 75–80
5. Vingerling, J. R., Hofman, A., Grobbee, D. E., and de Jong, P. T. (1996) Age-related macular degeneration and smoking. The Rotterdam Study. *Arch. Ophthalmol.* **114,** 1193–1196
6. Fine, S. L., Berger, J. W., Maguire, M. G., and Ho, A. C. (2000) Age-related macular degeneration. *N. Engl. J. Med.* **342,** 483–492
7. Marmor, M. F. (1975) Structure and function of the retinal pigment epithelium. *Int. Ophthalmol. Clin.* **15,** 115–130
8. Green, W. R. (1999) Histopathology of age-related macular degeneration. *Mol. Vis.* **5,** 27
9. Alcazar, O., Cousins, S. W., and Marin-Castaño, M. E. (2007) MMP-14 and TIMP-2 overexpression protects against hydroquinone-induced oxidant injury in RPE: implications for extracellular matrix turnover. *Invest. Ophthalmol. Vis. Sci.* **48,** 5662–5670
10. Espinosa-Heidmann, D. G., Suner, I. J., Catanuto, P., Hernandez, E. P., Marin-Castano, M. E., and Cousins, S. W. (2006) Cigarette smoke-related oxidants and the development of sub-RPE deposits in an experimental animal model of dry AMD. *Invest. Ophthalmol. Vis. Sci.* **47,** 729–737
11. Marin-Castaño, M. E., Striker, G. E., Alcazar, O., Catanuto, P., Espinosa-Heidmann, D. G., and Cousins, S. W. (2006) Repetitive nonlethal oxidant injury to retinal pigment epithelium decreased extracellular matrix turnover in vitro and induced sub-RPE deposits in vivo. *Invest. Ophthalmol. Vis. Sci.* **47,** 4098–4112
12. Strunnikova, N., Zhang, C., Teichberg, D., Cousins, S. W., Baffi, J., Becker, K. G., and Csaky, K. G. (2004) Survival of retinal pigment epithelium after exposure to prolonged oxidative injury: a detailed gene expression and cellular analysis. *Invest. Ophthalmol. Vis. Sci.* **45,** 3767–3777
13. Monks, T. J., and Jones, D. C. (2002) The metabolism and toxicity of quinones, quinonimines, quinone methides, and quinone-thioethers. *Curr. Drug Metab.* **3,** 425–438
14. DeCaprio, A. P. (1999) The toxicology of hydroquinone—relevance to occupational and environmental exposure. *Crit. Rev. Toxicol.* **29,** 283–330
15. Negi, A., and Marmor, M. F. (1984) Experimental serous retinal detachment and focal pigment epithelial damage. *Arch. Ophthalmol.* **102,** 445–449
16. Stein, J. M., and Luzio, J. P. (1991) Ectocytosis caused by sublytic autologous complement attack on human neutrophils. The sorting of endogenous plasma-membrane proteins and lipids into shed vesicles. *Biochem. J.* **274,** 381–386
17. Combes, V., Simon, A. C., Grau, G. E., Arnoux, D., Camoin, L., Sabatier, F., Mutin, M., Sanmarco, M., Sampol, J., and Dignat-George, F. (1999) In vitro generation of endothelial microparticles and possible prothrombotic activity in patients with lupus anticoagulant. *J. Clin. Investig.* **104,** 93–102
18. Sims, P. J., Faioni, E. M., Wiedmer, T., and Shattil, S. J. (1988) Complement proteins C5b-9 cause release of membrane vesicles from the platelet surface that are enriched in the membrane receptor for coagulation factor Va and express prothrombinase activity. *J. Biol. Chem.* **263,** 18205–18212
19. Iida, K., Whitlow, M. B., and Nussenzweig, V. (1991) Membrane vesiculation protects erythrocytes from destruction by complement. *J. Immunol.* **147,** 2638–2642
20. Pascual, M., Steiger, G., Sadallah, S., Paccaud, J. P., Carpentier, J. L., James, R., and Schifferli, J. A. (1994) Identification of membrane-bound CR1 (CD35) in human urine: evidence for its release by glomerular podocytes. *J. Exp. Med.* **179,** 889–899
21. Satta, N., Toti, F., Feugeas, O., Bohbot, A., Dachary-Prigent, J., Eschwège, V., Hedman, H., and Freyssinet, J. M. (1994) Monocyte vesiculation is a possible mechanism for dissemination of membrane-associated procoagulant activities and adhesion molecules after stimulation by lipopolysaccharide. *J. Immunol.* **153,** 3245–3255
22. Bütikofer, P., Kuypers, F. A., Xu, C. M., Chiu, D. T., and Lubin, B. (1989) Enrichment of two glycosyl-phosphatidylinositol-anchored proteins, acetylcholinesterase and decay accelerating factor, in vesicles released from human red blood cells. *Blood* **74,** 1481–1485
23. Jurianz, K., Ziegler, S., Donin, N., Reiter, Y., Fishelson, Z., and Kirschfink, M. (2001) K562 erythroleukemic cells are equipped with multiple mechanisms of resistance to lysis by complement. *Int. J. Cancer* **93,** 848–854
24. Miguet, L., Pacaud, K., Felden, C., Hugel, B., Martinez, M. C., Freyssinet, J. M., Herbrecht, R., Potier, N., van Dorsselaer, A., and Mauvieux, L. (2006) Proteomic analysis of malignant lymphocyte membrane microparticles using double ionization coverage optimization. *Proteomics* **6,** 153–171
25. Menegay, M., Lee, D., Tabbara, K. F., Cafaro, T. A., Urrets-Zavalía, J. A., Serra, H. M., and Bhattacharya, S. K. (2008) Proteomic analysis of climatic keratopathy droplets. *Invest. Ophthalmol. Vis. Sci.* **49,** 2829–2837
26. Sloley, S., Smith, S., Algeciras, M., Cavett, V., Busby, J. A., London, S., Clayton, D. F., and Bhattacharya, S. K. (2007) Proteomic analyses of songbird (zebra finch; Taeniopygia guttata) retina. *J. Proteome Res.* **6,** 1093–1100
27. Eng, J. K., McCormack, A. L., and Yates, J. R. (1994) An approach to correlate tandem mass spectral data of peptides with amino acid sequences in a protein database. *J. Am. Soc. Mass Spectrom.* **5,** 976–989
28. Patel, N., Solanki, E., Picciani, R., Cavett, V., Caldwell-Busby, J. A., and Bhattacharya, S. K. (2008) Strategies to recover proteins from ocular tissues for proteomics. *Proteomics* **8,** 1055–1070
29. Dunn, K. C., Aotaki-Keen, A. E., Putkey, F. R., and Hjelmeland, L. M. (1996) ARPE-19, a human retinal pigment epithelial cell line with differentiated properties. *Exp. Eye Res.* **62,** 155–169
30. Marler, P. (2004) Bird calls: their potential for behavioral neurobiology. *Ann. N.Y. Acad. Sci.* **1016,** 31–44
31. Weeks, R., Horwitz, B., Aziz-Sultan, A., Tian, B., Wessinger, C. M., Cohen, L. G., Hallett, M., and Rauschecker, J. P. (2000) A positron emission tomographic study of auditory localization in the congenitally blind. *J. Neurosci.* **20,** 2664–2672
32. Zhou, S., Bailey, M. J., Dunn, M. J., Preedy, V. R., and Emery, P. W. (2005) A quantitative investigation into the losses of proteins at different stages of a two-dimensional gel electrophoresis procedure. *Proteomics* **5,** 2739–2747
33. Young, R. W. (1987) Pathophysiology of age-related macular degeneration. *Surv. Ophthalmol.* **31,** 291–306
34. Spraul, C. W., and Grossniklaus, H. E. (1997) Characteristics of Drusen and Bruch's membrane in postmortem eyes with age-related macular degeneration. *Arch. Ophthalmol.* **115,** 267–273
35. Burns, R. P., and Feeney-Burns, L. (1980) Clinico-morphologic correlations of drusen of Bruch's membrane. *Trans. Am. Ophthalmol. Soc.* **78,** 206–225
36. Ishibashi, T., Patterson, R., Ohnishi, Y., Inomata, H., and Ryan, S. J. (1986) Formation of drusen in the human eye. *Am. J. Ophthalmol.* **101,** 342–353
37. Ishibashi, T., Sorgente, N., Patterson, R., and Ryan, S. J. (1986) Pathogenesis of drusen in the primate. *Invest. Ophthalmol. Vis. Sci.* **27,** 184–193
38. Zhu, Z. R., Goodnight, R., Nishimura, T., Sorgente, N., Ogden, T. E., and Ryan, S. J. (1988) Experimental changes resembling the pathology of drusen in Bruch's membrane in the rabbit. *Curr. Eye Res.* **7,** 581–592
39. Schulte, T., Paschke, K. A., Laessing, U., Lottspeich, F., and Stuermer, C. A. (1997) Reggie-1 and reggie-2, two cell surface proteins expressed

by retinal ganglion cells during axon regeneration. *Development* **124,** 577–587
40. Lang, D. M., Lommel, S., Jung, M., Ankerhold, R., Petrausch, B., Laessing, U., Wiechers, M. F., Plattner, H., and Stuermer, C. A. (1998) Identification of reggie-1 and reggie-2 as plasma membrane-associated proteins which cocluster with activated GPI-anchored cell adhesion molecules in non-caveolar micropatches in neurons. *J. Neurobiol.* **37,** 502–523
41. Simons, K., and Toomre, D. (2000) Lipid rafts and signal transduction. *Nat. Rev. Mol. Cell Biol.* **1,** 31–39
42. Anderson, R. G., and Jacobson, K. (2002) A role for lipid shells in targeting proteins to caveolae, rafts, and other lipid domains. *Science* **296,** 1821–1825
43. Simons, K., and Ikonen, E. (1997) Functional rafts in cell membranes. *Nature* **387,** 569–572
44. Hazarika, P., Dham, N., Patel, P., Cho, M., Weidner, D., Goldsmith, L., and Duvic, M. (1999) Flotillin 2 is distinct from epidermal surface antigen (ESA) and is associated with filopodia formation. *J. Cell. Biochem.* **75,** 147–159
45. Miyauchi, T., Kanekura, T., Yamaoka, A., Ozawa, M., Miyazawa, S., and Muramatsu, T. (1990) Basigin, a new, broadly distributed member of the immunoglobulin superfamily, has strong homology with both the immunoglobulin V domain and the beta-chain of major histocompatibility complex class II antigen. *J. Biochem.* **107,** 316–323
46. Fadool, J. M., and Linser, P. J. (1993) Differential glycosylation of the 5A11/HT7 antigen by neural retina and epithelial tissues in the chicken. *J. Neurochem.* **60,** 1354–1364
47. Muramatsu, T., and Miyauchi, T. (2003) Basigin (CD147): a multifunctional transmembrane protein involved in reproduction, neural function, inflammation and tumor invasion. *Histol. Histopathol.* **18,** 981–987
48. Yan, L., Zucker, S., and Toole, B. P. (2005) Roles of the multifunctional glycoprotein, emmprin (basigin; CD147), in tumour progression. *Thromb. Haemost.* **93,** 199–204
49. Nabeshima, K., Iwasaki, H., Koga, K., Hojo, H., Suzumiya, J., and Kikuchi, M. (2006) Emmprin (basigin/CD147): matrix metalloproteinase modulator and multifunctional cell recognition molecule that plays a critical role in cancer progression. *Pathol. Int.* **56,** 359–367
50. Gabison, E. E., Hoang-Xuan, T., Mauviel, A., and Menashi, S. (2005) EMMPRIN/CD147, an MMP modulator in cancer, development and tissue repair. *Biochimie* **87,** 361–368
51. Kanekura, T., Chen, X., and Kanzaki, T. (2002) Basigin (CD147) is expressed on melanoma cells and induces tumor cell invasion by stimulating production of matrix metalloproteinases by fibroblasts. *Int. J. Cancer* **99,** 520–528
52. Kataoka, H., DeCastro, R., Zucker, S., and Biswas, C. (1993) Tumor cell-derived collagenase-stimulatory factor increases expression of interstitial collagenase, stromelysin, and 72-kDa gelatinase. *Cancer Res.* **53,** 3154–3158
53. Guo, H., Zucker, S., Gordon, M. K., Toole, B. P., and Biswas, C. (1997) Stimulation of matrix metalloproteinase production by recombinant extracellular matrix metalloproteinase inducer from transfected Chinese hamster ovary cells. *J. Biol. Chem.* **272,** 24–27
54. Sameshima, T., Nabeshima, K., Toole, B. P., Yokogami, K., Okada, Y., Goya, T., Koono, M., and Wakisaka, S. (2000) Glioma cell extracellular matrix metalloproteinase inducer (EMMPRIN) (CD147) stimulates production of membrane-type matrix metalloproteinases and activated gelatinase A in co-cultures with brain-derived fibroblasts. *Cancer Lett.* **157,** 177–184
55. Yang, J. M., Xu, Z., Wu, H., Zhu, H., Wu, X., and Hait, W. N. (2003) Overexpression of extracellular matrix metalloproteinase inducer in multidrug resistant cancer cells. *Mol. Cancer Res.* **1,** 420–427
56. Sun, J., and Hemler, M. E. (2001) Regulation of MMP-1 and MMP-2 production through CD147/extracellular matrix metalloproteinase inducer interactions. *Cancer Res.* **61,** 2276–2281
57. Sidhu, S. S., Mengistab, A. T., Tauscher, A. N., LaVail, J., and Basbaum, C. (2004) The microvesicle as a vehicle for EMMPRIN in tumor-stromal interactions. *Oncogene* **23,** 956–963
58. Egawa, N., Koshikawa, N., Tomari, T., Nabeshima, K., Isobe, T., and Seiki, M. (2006) Membrane type 1 matrix metalloproteinase (MT1-MMP/MMP-14) cleaves and releases a 22-kDa extracellular matrix metalloproteinase inducer (EMMPRIN) fragment from tumor cells. *J. Biol. Chem.* **281,** 37576–37585
59. Annabi, B., Lachambre, M., Bousquet-Gagnon, N., Pagé, M., Gingras, D., and Béliveau, R. (2001) Localization of membrane-type 1 matrix metalloproteinase in caveolae membrane domains. *Biochem. J.* **353,** 547–553
60. Puyraimond, A., Fridman, R., Lemesle, M., Arbeille, B., and Menashi, S. (2001) MMP-2 colocalizes with caveolae on the surface of endothelial cells. *Exp. Cell Res.* **262,** 28–36
61. Gálvez, B. G., Matías-Román, S., Yáñez-Mó, M., Vicente-Manzanares, M., Sánchez-Madrid, F., and Arroyo, A. G. (2004) Caveolae are a novel pathway for membrane-type 1 matrix metalloproteinase traffic in human endothelial cells. *Mol. Biol. Cell* **15,** 678–687
62. Maecker, H. T., Todd, S. C., and Levy, S. (1997) The tetraspanin superfamily: molecular facilitators. *FASEB J.* **11,** 428–442
63. Boucheix, C., and Rubinstein, E. (2001) Tetraspanins. *Cell. Mol. Life Sci.* **58,** 1189–1205
64. Hemler, M. E. (2003) Tetraspanin proteins mediate cellular penetration, invasion, and fusion events and define a novel type of membrane microdomain. *Annu. Rev. Cell Dev. Biol.* **19,** 397–422
65. Levy, S., and Shoham, T. (2005) The tetraspanin web modulates immune-signalling complexes. *Nat. Rev. Immunol.* **5,** 136–148